EBioMedicine 62 (2020) 103120

Contents lists available at ScienceDirect

EBioMedicine

journal homepage: www.elsevier.com/locate/ebiom

Research paper

hESC-derived immune suppressive dendritic cells induce immune tolerance of parental hESC-derived allografts

Dilyana Todorova[a], Yue Zhang[b], Qu Chen[c], Jingfeng Liu[a], Jingjin He[c], Xuemei Fu[c,d,*], Yang Xu[a,b,c,**]

[a] Division of Biological Sciences, University of California, San Diego, 9500 Gilman Drive, La Jolla, CA 92093, USA
[b] Guangzhou University of Chinese Medicine, Second Clinical Medical College, 232 Waihuan Road E, Guangzhou, Guangdong 510006, China
[c] The Eighth Affiliated Hospital, Sun Yat-sen University, Shenzhen, Guangdong 518033, China
[d] Shenzhen Children's Hospital, Shenzhen 518026, China.

ARTICLE INFO

Article History:
Received 6 June 2020
Revised 28 September 2020
Accepted 26 October 2020
Available online xxx

Keywords:
Human embryonic stem cells
Allogeneic immune rejection
Immune tolerance
Dendritic cells
Regulatory T cells
Immune system humanized mice

ABSTRACT

Background: With their inherent capability of unlimited self-renewal and unique potential to differentiate into functional cells of the three germ layers, human embryonic stem cells (hESCs) hold great potential in regenerative medicine. A major challenge in the application of hESC-based cell therapy is the allogeneic immune rejection of hESC-derived allografts.
Methods: We derived dendritic cell-like cells (DCLs) from wild type and CTLA4-Ig/PD-L1 knock-in hESCs, denoted WT DCLs and CP DCLs. The expression of DC-related genes and surface molecules was evaluated, as well as their DCL capacity to stimulate allogeneic T cells and induce regulatory T (Treg) cells *in vitro*. Using an immune system humanized mouse model, we investigated whether the adoptive transfer of CP DCLs can induce long-term immune tolerance of parental hESC-derived smooth muscle and cardiomyocyte allografts.
Findings: CP DCLs can maintain immune suppressive properties after robust inflammatory stimulation and induce Treg cells. While CP DCLs survive transiently *in vivo*, they induce long-term immune tolerance of parental hESC-derived allografts.
Interpretation: This strategy does not cause systemic immune suppression but induces immune tolerance specific for DCL-specific HLAs, and thus it presents a safe and effective approach to induce immune tolerance of allografts derived from any clinically approved hESC line.
Funding: NSFC, leading talents of Guangdong Province Program (No. 00201516), Key R&D Program of Guangdong Province (2019B020235003), Science and Technology Innovation Committee of Shenzhen Municipality (JCYJ20180504170301309), National High-tech R&D Program (863 Program No. 2015AA020310), Shenzhen "Sanming" Project of Medicine (SZSM201602102), Development and Reform Commission of Shenzhen Municipality (S2016004730009), CIRM (DISC2–10559).

1. Introduction

Human pluripotent stem cells (hPSCs), including human embryonic stem cells (hESCs) and induced pluripotent stem cells (hiPSCs), have the unique potential to generate an unlimited cell source for tissue regeneration. During the past two decades, considerable progress has been achieved in developing technologies to efficiently differentiate hPSCs into functional lineage-specific cells [1–6]. In addition, clinical trials of hESC-based cell therapy have been initiated in patients with spinal cord injury, macular dystrophy, severe ischemic left ventricular dysfunction, and type 1 diabetes [7–9]. Although the reprogramming technologies allow the generation of patient-specific hiPSCs, the development of hiPSC-based personalized therapy faces considerable challenges that are associated with high cost, increased risk of genetic mutations, and uncertain quality [10,11]. In addition, accumulating data indicate that certain autologous iPSCs-derived cells are not inherently immunologically silent and can be rejected by the syngeneic immune system [12–14].

One of the major obstacles that hamper the clinical application of hESC-based therapies is the immune rejection of the hESC-derived allografts by the recipient [15]. While effective, current immunosuppressive drugs are highly toxic to patients with chronic diseases and cause serious side effects, such as increased risk of spontaneous

* Corresponding author at: The Eighth Affiliated Hospital, Sun Yat-sen University, Shenzhen, Guangdong 518033, China.
** Corresponding author at: Division of Biological Sciences, University of California, San Diego, 9500 Gilman Drive, La Jolla, CA 92093, USA.
E-mail addresses: fxmzj2004@163.com (X. Fu), yangxu@ucsd.edu (Y. Xu).

https://doi.org/10.1016/j.ebiom.2020.103120

Research in context

Evidence before this study

Despite significant progress in developing hESC-based therapies to treat major human diseases, one of the key challenges remains the allogeneic immune rejection of hESC-derived allografts.

Various strategies have been published to prevent allogeneic immune rejection of hESC-derived allografts, such as antibody-mediated blockade or direct gene-editing of the hESCs. However, these approaches pose the risk of systemic immune suppression or renders the hESC-derived allografts immune evasive and susceptible to infection and cancer.

Added value of this study

To develop a safe and effective approach to induce immune tolerance of hESC-derived allografts without the safety risk associated with previous approaches, we took advantage of the well-known capability of immature DCs to induce immune tolerance of antigen-specific T cells. We demonstrate that CTLA4-Ig/PD-L1 expressing DCLs derived from hESCs (CP DCLs) can induce persistent immune tolerance of the parental hESC-derived allografts. In contrast to normal immature DCs, CP DCLs maintain immature and tolerogenic properties even after strong inflammatory stimuli. While CP DCLs survive transiently *in vivo*, they can induce long-term immune tolerance of parental hESC-derived allografts. This reduces the cancer risk of the genetically modified CP DCLs as well as parental hESC-derived allografts that remain under immune surveillance. In this context, only T cells specific for the DCL-expressing alloantigens are immune tolerated, while other T cells remain able to mount immune responses to antigens produced during infection or cellular transformation.

Implications of all the available evidence

When compared to the published immune protection strategies, our approach will not lead to systemic immune suppression nor immune evasive allografts, and thus mitigate the cancer and infection risk associated with existing approaches. Based on the findings that CP DCLs can induce immune tolerance of various functional cell types derived from the same strain of hESCs, our approach should improve the feasibility for clinical development of hESC-based therapy. In this context, for each clinically approved hESC cell line, the development of CP hESC-derived DCLs can be universally applied to induce immune tolerance of various hESC-derived functional cells to treat major human diseases.

infection, nephrotoxicity, and cancer [16]. Different approaches have been developed to achieve immune protection of hESC-derived allografts with the least impact on the survival and function of the transplanted cells. For example, antibody-mediated coreceptor and costimulation blockade can achieve tolerance of hESC-derived xenografts in the context of mouse immune system [17,18]. By genetic modification of hESCs that induces the expression of immune suppressive molecules such as programmed death ligand-1 (PD-L1) and CTLA4 immunoglobulin fusion protein (CTLA4-Ig), or that disrupts the expression of major histocompatibility complex (MHC) class I and class II molecules, show promising results in protecting allografts from allogeneic T cells [19–21]. Using a humanized mouse (Hu-mouse) model with functional human immune system that can robustly reject allogeneic hESC-derived allografts [22], it has been shown that the simultaneous expression of CTLA4-Ig and PD-L1 protects CP hESC-derived cells from allogeneic immune rejection [22]. CTLA4 and PD-L1 are critical molecules that shut down T-cell activation, culminating in T-cell death or anergy [23,24]. Because CTLA4 binds CD80 and CD86 with higher affinity than CD28, CTLA4-Ig has been developed to block the costimulatory signal and inhibit T-cell mediated immune response [25]. However, transplanted cells that were engineered to escape immune surveillance may pose long-term risk of uncontrollable cellular transformation or impaired viral clearance.

By their capacity to sense and integrate stimulating or tolerogenic signals from the peripheral and lymphoid tissues, dendritic cells (DCs) play a central role in the maintenance of immune homeostasis. Depending on the context in which antigen presentation occurs, DCs can either induce robust immunity or promote and maintain immune tolerance [26]. Optimal T cell activation requires several signals: recognition of the antigenic peptide bound to MHC molecules by a specific T-cell receptor (TCR), co-stimulation of CD28 by the molecules of the B7-receptor families expressed on antigen-presenting cells, and the production of T cell stimulatory cytokines. The balance between the expression of inhibitory and stimulatory ligands by DCs regulates the outcome of their interactions with T cells [23]. In this context, co-stimulatory signals are required for efficient T cell activation, and TCR ligation without co-stimulation can induce T-cell anergy or apoptosis [27]. Therefore, it has been hypothesized that the administration of immature DCs expressing allo-HLAs but with low expression of co-stimulatory molecules could be used to prevent transplant rejection [28]. One of the main bottlenecks in achieving this goal is that immature DCs can be activated and become stimulatory *in vivo* after encountering different inflammatory factors and lose their tolerogenic properties.

For more than 20 years, considerable effort has been made to generate potential donor- or recipient-derived tolerogenic DCs, which have been tested in transplantation models [26,29,30]. One approach is to treat monocyte-derived DCs with a variety of pharmaceutical agents or RNA interference to maintain their immature phenotype, so that they express low levels of co-stimulatory molecules and induce anergy in antigen-specific T cells [31–34]. The genetic modification of DCs was another approach to generate tolerogenic DCs. For example, donor-derived murine myeloid DCs engineered to overexpress Fas ligand or CTLA4-Ig could promote cardiac allograft survival in mouse models [35,36]. Based on studies in rodents and non-human primates [37], the first-in-human study of donor-derived regulatory DCs was initiated in liver transplant recipients to evaluate the safety and the efficacy of the infused cells to achieve early complete immunosuppression withdrawal [38]. Recently, the generation of DCs with tolerogenic properties was reported from mouse and human iPSCs [39,40]. However, the tolerogenic potential of human iPSC- derived DCs was only tested *in vitro* and the efficacy of these DCs to suppress human allogeneic immune response *in vivo* has not been tested.

To overcome the key challenge that immature tolerogenic DCs can be activated by inflammatory stimuli *in vivo* and lose their tolerogenic property, we hypothesized that DCs derived from CTLA4-Ig/PD-L1-expressing hESCs can maintain immune suppressive properties *in vivo* and induce immune tolerance of the allogenic cells derived from parental hESCs. Here we demonstrate that DC-like cells (DCLs) derived from CP hESCs, denoted CP DCLs, can maintain immune suppressive characteristics and induce regulatory T (Treg) cells. Using an immune system humanized model, we show that the adoptive transfer of CP DCLs before the transplantation of parental hESC-derived allografts can protect these allografts from immune rejection by inducing immune tolerance.

2. Methods

2.1. Cell culture

The Hues3 hESC (RRID:CVCL_B161) line was cultured on CF-1 mouse embryonic fibroblast feeder layer in knockout Dulbecco`s

modified Eagle`s medium (DMEM) supplemented with 10% knockout serum replacement, 10% plasmanate (Grifols therapeutic), 0.1 mM nonessential amino acids, 2 mM Glutamax, 1% penicillin/streptomycin, 10 ng/ml basic fibroblast growth factor, 55 μM β-mercaptoethanol. The H1 (RRID:CVCL_9771) and H9 (RRID:CVCL_9773) hESC lines were cultured on mouse embryonic fibroblast feeder layer in DMEM/F12 medium supplemented with 20% knockout serum replacement, 0.1 mM nonessential amino acids, 2 mM Glutamax, 1% penicillin/streptomycin, 10 ng/ml basic fibroblast growth factor, 55 μM β-mercaptoethanol. The hESCs were dissociated with TrypLE and passaged on feeders with 1:10 dilution. All reagents were purchased from Life Technologies unless indicated elsewhere. The CTLA4-Ig/PDL1 knock-in hESCs were generated using BAC-based homologous recombination as previously described [22]. The hESCs were tested for mycoplasma contamination using the MycoAlert Plus kit (Lonza Cat#LT07−703). This work was approved by the Institutional Embryonic Stem Cell Research Oversight Committee and Human Research Protection Program.

2.2. Differentiation of hESCs into DCLs

DCL differentiation from hESCs was conducted using OP9 feeders according to previously published protocols [5,41] (Fig. 1a). Undifferentiated hESCs maintained on CF-1 mouse embryonic fibroblasts were harvested using collagenase type IV 0.1% and cultured on OP9 (RRID:CVCL_KB57) feeder cell layers for 6 days in α-minimum essential medium (MEM-α) supplemented with 20% HyClone characterized FBS (GE Healthcare Cat#SH30071.03). On day 6, the cells were dissociated with trypsin/EDTA 0.05%, plated on fresh OP9 feeders and cultured for additional 12 days. On day 18, the cells were dissociated using collagenase type IV 0.1%, followed by treatment with trypsin/EDTA 0.05%/DNAase I 0.1%. The dissociated cells were plated onto culture dishes, incubated overnight and the floating cells were collected. The floating cells were passed through nylon meshes (Cell strainer, 100 μm, BD Falcon) and cultured for 10−14 days in MEM-α 20% characterized FBS containing GM-CSF (100 ng/ml, PeproTech Cat#300−03). To generate DCLs, the cells were further cultured in presence of GM-CSF (100 ng/ml) and Il-4 (100 ng/ml, PeproTech Cat#200−04) for 7 days in RPMI-1640 medium (Life Technologies) containing 10% FCS, 10 mM HEPES, 2 mM Glutamax, 1 mM sodium pyruvate, 1% penicillin/streptomycin, and 55 μM β-mercaptoethanol. To activate DCLs, the cells were further incubated for 2−3 days with TNF-α (10 ng/ml, PeproTech Cat#300−01A) and LPS (1 μg/ml, Sigma-Aldrich Cat#L5543).

2.3. Differentiation of hESCs into cardiomyocytes and smooth muscle cells

Cardiomyocyte differentiation was performed as previously described [1]. hESCs were plated on matrigel-coated plates, when the culture reached confluence, cells were treated with GSK3 inhibitor CHIR99021(Selleckchem Cat#2924) in RPMI/B27-insulin (without insulin) for 24 h (day 0 to day 1). The next day, the medium was changed to RPMI/B27-insulin for 2 days. On day 3, the cells were treated with IWP4 (Stemgent Cat#04−0036) for 2 days. From day 7, the medium was changed to RPMI/B27 with medium change every other day.

The directed differentiation of hESCs into SMCs was performed as previously described [42]. Briefly, the hESCs were separated from the feeder cells and plated on 6 well gelatin-coated culture plates (Becton Dickinson). Cells were maintained daily in differentiation media consisting of DMEM (Invitrogen), 15% HyClone characterized FBS (GE Healthcare Cat#SH30071.03), 2 mM l-glutamine (Invitrogen), 1 mM MTG (Sigma), 1% nonessential amino acids (Invitrogen), pen/strep (Invitrogen), and 10 μM all trans retinoic acid (Sigma) for 10 days. Cells were then continued to differentiate in serum-free culture medium, consisting of knock-out DMEM (Invitrogen), 15% knock-out serum replacement (Invitrogen), 2 mM l-glutamine, 1 mM MTG, 1% nonessential amino acids, penicillin, and streptomycin for another 10 days.

2.4. Generation of Hu-mice with functional immune system

All mouse work was approved by the Institutional Animal Care and Use Committee and performed in the dedicated procedure room in the animal facility according to the animal protocol. NSG (NOD.Cg-Prkdc^{scid} Il2rg^{tm1Wjl}/SzJ) immunodeficient mice of 6−8 weeks of age were purchased from the Jackson Laboratory, were housed in the animal facility in groups of up to five animals/cage under 12-hr light/dark cycles and allowed to acclimate for 7 days before surgery. Human fetal liver and thymus tissues of gestational age of 17 to 20 weeks were obtained from Advanced Bioscience Resource and CD34$^+$ cells were isolated from human fetal liver tissues by magnetic cell sorting using anti-human CD34 microbeads (Miltenyi Biotec Cat#130−046−702). The Hu-mice with functional immune system were generated as previously described [22,43]. After a sublethal total body irradiation (2.25 Gy), NSG mice were transplanted with a human fetal thymus piece of about 1mm^3 under the kidney capsule and intravenously transfused with 1×10^5 CD34$^+$ human fetal liver cells. The reconstitution of the mice with functional immune system was assessed 2 months later by Flow Cytometry. Each batch of Hu-mice was composed of mice with same age, same sex, and was generated with the same batch of human fetal thymus and CD34$^+$ human fetal liver cells. Each mouse was assigned a number. Before performing the animal experiments, the reconstitution with human immune cells of all mice was checked by flow cytometry and only mice with similar levels of human immune reconstitution were used in each set of experiment. After this initial assessment, in each set of experiment, the mice were randomly included in each group, using a computer-based random number generator.

2.5. Adoptive transfer of DCLs and transplantation experiments

DCLs were intravenously infused in Hu-mice 7 days before the transplantation of hESCs, hESCs-derived cardiomyocytes or SMCs. 1×10^6 DCLs in 500μl PBS were injected in the tail vein using 27 G needle. Human ESCs were harvested, washed with PBS, 3×10^6 cells were suspended in PBS containing 30%(V/V) Matrigel (BD Biosciences Cat#BD354277) and subcutaneously implanted in NSG and Hu-mice. Cardiomyocytes and SMCs differentiated from hESCs were harvested, washed with PBS, suspended in PBS containing 50% Matrigel and intramuscularly implanted into the hind leg gastrocnemius with a 20 G needle.

Mouse experimental groups were sized at $n \geq 4$, based on data generated in previous studies [14,22].All the samples/ animals analysed were included in the data and none was excluded. For each experiment, the exact number of mice (n) used is stated in the respective figure legend. In each set of experiment, age- and sex-matched mice were randomly included in each group, using a computer-based random number generator. Age- and sex-matched NSG mice were used as control in each experiment. The adoptive transfer of DCLs and the transplantation experiments were performed by the same operator to minimize potential confounders, the researcher was blinded to experimental groups during the transplantation experiments. At different time-points after transplantation, as specified in the relative figure legend and result section, the grafts were collected and analyzed for graft survival and immune cell infiltration. The assessment of the outcome was not blinded.

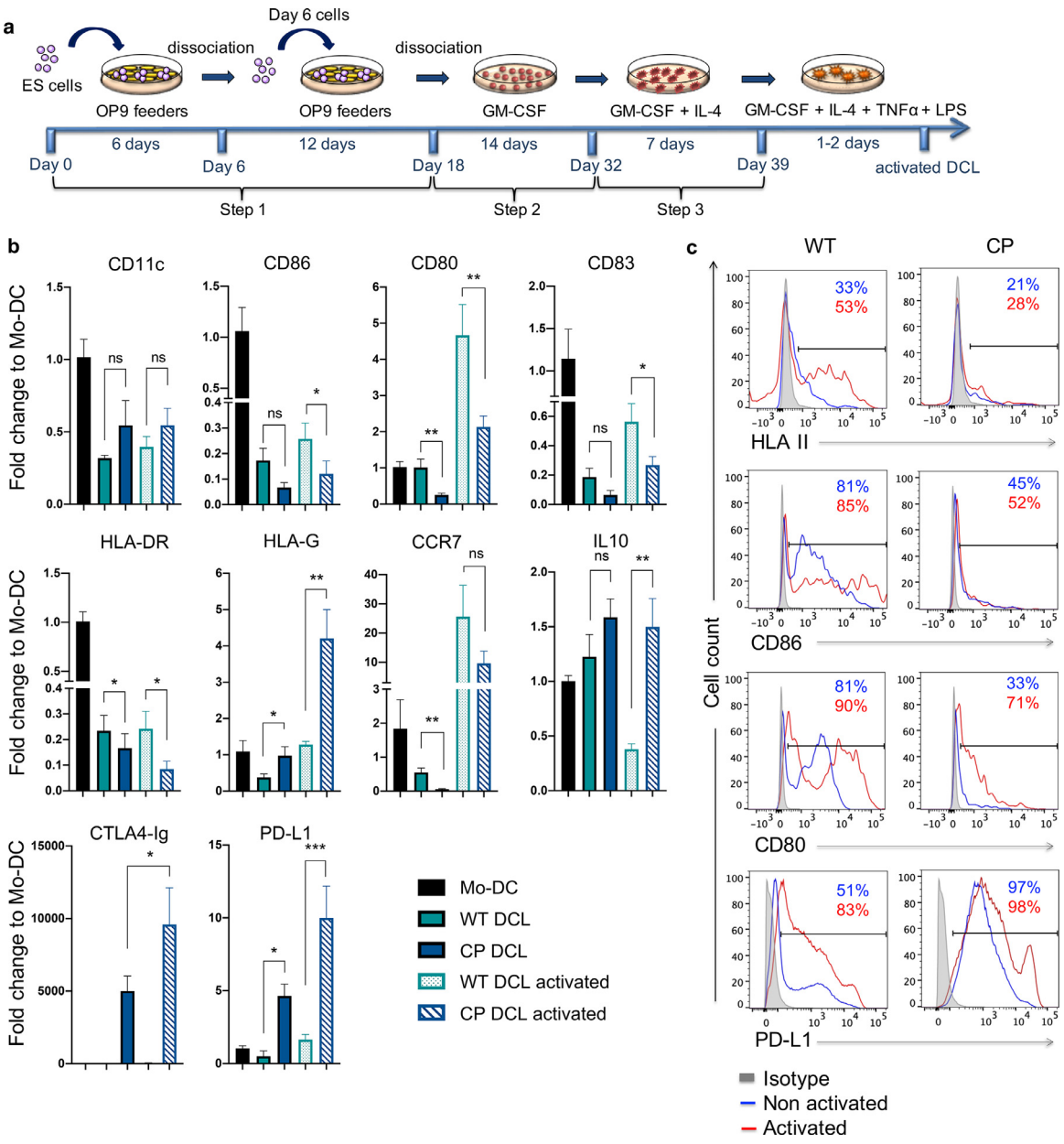

Fig. 1. DCL cells differentiated from CP hESCs cannot be activated by TNF-α and LPS. (a) Schematic description of the differentiation protocol of hESCs into DCL cells. (b) The expression of DC-specific genes was evaluated at the end of step 3 of the differentiation protocol of WT and CP hESCs with or without TNF-α + LPS activation. The gene expression of DCLs was normalized to the gene expression of monocyte-derived DC (Mo-DC). Data are presented as mean values ± SEM (n = 6). Data from different groups were compared using one-way ANOVA test, *, ** and *** denote significant differences at $P<0.05$, $P<0.01$ and $P<0.001$ respectively, ns denotes non-significant. (c) The expression of MHC II, CD86, CD80 and PDL1 was evaluated by flow cytometry at the end of step 3 of differentiation before (blue line) and after TNF-α + LPS activation (red line), the isotype control is shown in gray.

2.6. In vivo tracking of DCLs

WT and CP DCLs were labeled with 5 μM CFDA using Vybrant CFDA SE cell tracer kit (Molecular probes Cat# V12883) according to the manufacturer instruction. After labeling, the cells were washed 2 times with PBS and 1×10^6 DCLs in 500μl PBS were injected in the tail vein of Hu-mice using 27 G needle. Two days, seven days and ten days after injection, the blood, spleen and thymus were collected, single cell suspension was prepared and analyzed by flow cytometry for the presence of CFDA-labeled DCLs. Hu-mice that didn`t receive any DCL cells were served as controls.

2.7. Quantitative real-time PCR analysis

Total RNA was extracted from hESCs, hESCs-derived DCs and from teratomas formed by hESCs using RNA isolation kit (Qiagen). Total RNA (1 μg) was reversely transcribed into cDNA, using cDNA transcription kit (Applied Biosystems Cat#4368814) and followed by quantitative real time PCR analysis using the PowerUp™ SYBR™ Green Master Mix (Applied Biosystems Cat# A25742) and StepOne Plus RealTime PCR System (Applied Biosystems). The primers used are listed in Supplemental Table S1.

2.8. Immunohistochemistry

For immunofluorescence staining, teratomas, cardiomyocyte- and SMC- grafts were frozen in optimal cutting temperature (OCT) compound (Sakura Finetek) and sectioned on a cryostat at a thickness of 8 μm. Frozen sections were fixed for 15 min with 4% paraformaldehyde solution in PBS (Affimetrix), permeabilized for 10 min with 0.3% Triton X-100 (Sigma), blocked for 30 min with PBS containing 1% BSA, 0.05% tween 20, and incubated with primary antibodies

overnight at 4 °C. Antibodies used were as following: mouse anti-human CD3 (Thermo Fisher Scientific Cat# 16−0038−85, RRID: AB_468,857), rabbit anti-human CD3 (Agilent Cat# A0452, RRID: AB_2,335,677), mouse anti-human CD4 (BD Biosciences Cat# 550,369, RRID:AB_393,640), mouse anti-human CD8 (BD Biosciences Cat# 555,364, RRID:AB_395,767), mouse anti-human Foxp3 (Thermo Fisher Scientific Cat# 14−4777−82, RRID:AB_467,556), rabbit anti-human cardiac troponin I (Abcam Cat# ab52862, RRID:AB_869,983), rabbit anti-human SM22 (Abcam Cat# ab14106, RRID:AB_443,021). The sections were washed with PBS, incubated for 45 min with the corresponding conjugated secondary antibodies. The secondary antibodies used are the following: goat anti-mouse AlexaFluor488 (Thermo Fisher Scientific Cat# A-11,001, RRID:AB_2,534,069), goat anti-rabbit AlexaFluor488 (Molecular Probes Cat# A-11,008, RRID: AB_143,165), goat anti-mouse AlexaFluor568 (Molecular Probes Cat# A-11,031, RRID:AB_144,696), goat anti-rabbit AlexaFluor568 (Molecular Probes Cat# A-11,011, RRID:AB_143,157). After incubation, the sections were washed with PBS and slides were mounted with mounting medium for fluorescence with Dapi (Vector Laboratories Cat# H-1200, RRID:AB_2,336,790). Images were captured using Leica SP8 Confocal microscope and Zeiss Axiovert 40 CFL Inverted microscope.

2.9. Flow cytometry

For the characterization of DCLs, cardiomyocytes and SMCs differentiated from hESCs by flow cytometry, 5×10^5 cells were washed with PBS 2% FBS, incubated with the cell-type specific antibodies for 30 min at 4 °C. For intracytoplasmic staining, cells were fixed and permeabilized using Cytofix/Cytoperm Fixation/Permeabilization solution kit (BD Pharmingen). The antibodies used were as follows: For DCLs characterization, FITC-anti-HLADR, DQ, DP (BD Biosciences Cat# 550,853, RRID:AB_393,926), PE-anti-hCD80 (BD Biosciences Cat# 557,227, RRID:AB_396,606), PE-anti-hCD86 (BD Biosciences Cat# 555,658, RRID:AB_396,013), APC-anti-hCD45 (BD Biosciences Cat# 555,485, RRID:AB_398,600), FITC-anti-hCD43 (BD Biosciences Cat# 560,978, RRID:AB_10,562,394), BV421-anti-hCD11c (BioLegend Cat# 337,225, RRID:AB_2,564,484), PE-anti-HLAG (Thermo Fisher Scientific Cat# 12−9957−41, RRID:AB_11,151,694), PE-anti-HLA ABC (Thermo Fisher Scientific Cat# 12−9983−42, RRID:AB_10,547,062), PerCP-eFluor710-anti-hCTLA-4 (Thermo Fisher Scientific Cat# 46−1529−42, RRID:AB_2,573,718); For SMCs, FITC-anti-human Smooth muscle actin (Sigma-Aldrich Cat# F3777, RRID:AB_476,977); For cardiomyocytes, mouse anti-human cardiac troponin T (Lab Vision Cat# MS-295-P, RRID:AB_61,806), followed by incubation with anti-mouse Alexa Fluor 568.

For flow cytometric analysis of teratomas, teratomas were dissociated using a mixture of liberase blendzyme TM/liberase blendzyme TH (Roche Cat# 5,401,119,001 and Cat# 5,401,135,001) and DNAse I (STEMCELL Technologies Cat# 07,900). After dissociation, the cell suspension was passed through nylon meshes (Cell strainer, 40 μm, BD Falcon), washed with PBS and red blood cells were removed with ACK lysis buffer. Cells were stained with the following antibodies: APC-anti-hCD45, APC—Cy7-anti-hCD14 (BD Biosciences Cat# 557,831, RRID:AB_396,889), PE-Cy7-anti-hCD3 (BioLegend Cat# 300,420, RRID:AB_439,781), PerCp-Cy5.5-anti-hCD19 (BioLegend Cat# 302,229, RRID:AB_2,275,547).

For flow cytometric analysis of blood, spleen, thymus and bone-marrow of Hu-mice, single-cell suspension was prepared and red blood cells in samples were removed with ACK lysis buffer. The cells were incubated with the following antibodies: FITC-anti-hCD8 (BD Biosciences Cat# 555,635, RRID:AB_395,997), PE-anti-hCD4 (BD Biosciences Cat# 555,347, RRID:AB_395,752), APC-anti-hCD45, PE-Cy7-anti-hCD3, BV711-anti-hCD19 (BioLegend Cat# 363,021, RRID: AB_2,564,230). After staining, the cells were analyzed with BD LSR-II (Becton Dickinson) or ZE5 (BioRad) flow cytometers.

2.10. ELISA

The secretion of CTLA4-Ig by CP DCLa was assessed using Human CTLA4 ELISA kit (Novus Cat#NBP1−91,268). 2.5×10^6 WT or CP DCLs were cultured in 2.5 ml of culture media for 48 h, the media was collected, after centrifugation at 300 g for 5 min the supernatants were collected and analyzed for the presence of CTLA4-Ig by ELISA according to the manufacturer`s instructions.

2.11. T cell proliferation and activation assays

Allogeneic T cells from spleens of Hu-mice were isolated using human CD4 (Miltenui Cat#130−045−101) and CD8 T cell isolation kit (Miltenyi Cat# 130−045−201). The isolated T cells were labeled with 5μM CFSE (Biolegend Cat# 422,701). Briefly, 5×10^5 T cells were co-cultured for 5 days with 1.25×10^5 DCLs differentiated from WT and CP ESCs. After co-culture, cells were stained with PE-anti-hCD4 or PE-anti-hCD8 antibody and the proliferation of the T cells was assessed by the loss of CFSE signal using flow cytometry (ZE5 BioRad).

For CD8 T cell activation assay, allogeneic CD8 cells were isolated from the spleen of Hu-mice using CD8 T cell isolation kit. 5×10^5 T cells were co-cultured for 5 days with 1.25×10^5 DCLs differentiated from WT and CP ESCs. At the end of the co-culture, the cells were stained with FITC-anti-hCD8 and BV650-anti-hCD62L (BD Biosciences Cat# 563,808, RRID:AB_2,738,433) and the surface expression of CD62L by $CD8^+$ *T* cells was assessed by flow cytometry.

2.12. Treg assay

Allogeneic $CD4^+$ T cells were isolated from the spleen of Hu-mice using CD4 T cell isolation kit. 5×10^5 T cells were co-cultured for 7 days with 1.25×10^5 DCLs differentiated from WT and CP ESCs. At the end of the co-culture, the cells were stained with BV421-anti-hCD25 (BioLegend Cat# 302,629, RRID:AB_10,896,914), BV711-anti-hLAG3 (BioLegend Cat# 369,319, RRID:AB_2,716,124), PE-anti-hCD4, APC-anti-hPD1 (BioLegend Cat# 329,908, RRID:AB_940,475), PerCP-eFluor710-anti-hCTLA4. After extracellular staining, the cells were fixed and permeabilized using Cytofix/Cytoperm Fixation/Permeabilization solution kit (BD Pharmingen Cat# 554,715) and stained with Alexa488-anti-hFoxp3 (BD Biosciences Cat# 560,887, RRID: AB_10,562,196).The percentage of $CD25^{high}Foxp3^+$ $CD4^+$ T cells and the expression of CTLA4, LAG3 and PD1 by $CD25^{high}Foxp3^+$ $CD4^+$ T cells was assessed by flow cytometry.

2.13. Ethics

All animal experiments were approved by Institutional Animal Care and Use Committee (IACUC) (Protocol # S09182). hESC work was approved by Institutional Human Research Protections Program (IRB # 180,065).

2.14. Statistics

The continuous variables were tested for normal distribution with Shapiro-Wilk normality test. For non-normally distributed variables, when 2 groups were analyzed, the medians of non normally distributed variable were compared using non-parametric Mann-Whitney test. When more than 2 groups were analyzed, the medians were compared using non-parametric Kruskal-Wallis test with Dunn`s multiple comparisons test. For normally distributed variables, data from different groups were compared using one-way ANOVA test. Data were analyzed using GraphPad Prism version 8.0 (GraphPad Software Inc. La Jolla). Results were considered statistically significant when $p < 0.05$.

2.15. Role of funding source

The funders have no role in this study design, data collection, data analysis, interpretation, or writing of the report.

3. Results

3.1. Dendritic cell-like cells (DCLs) differentiated from CP hESCs exhibit immune suppressive characteristics

Using BAC-based targeting vector, we previously reported the generation of CTLA4-Ig and PD-L1 knock-in hESCs (termed CP hESCs, Fig. S1a) that constitutively express CTLA4-Ig and PD-L1 in all derivatives [22]. To investigate the impact of CP expression on the differentiation of hESCs into DCLs, we used the protocol established by Senju et al. with minor modifications (Fig. 1a) [5]. At the end of step 2 of the differentiation protocol that corresponds to the generation of hematopoietic progenitors, both WT and CP hESCs were able to differentiate into $CD43^+CD45^+$ hematopoietic progenitors with similar efficiency, approximately 97% (Fig. S1b). At the end of step 3, the expression of CD11c by hESC-derived DCLs (Fig.S1d) was comparable to that of monocyte-derived DC (Mo-DC) (Fig. S2a). The differentiation efficiency of WT and CP hESCs into DCLs was similar, both resulting in approximately 95% of $CD11c^+$ cells at the end of step 3 (Fig. S1d). These data indicate that CP expression did not affect the differentiation efficiency of hESCs into DCLs.

The overall expression of DC-related genes seems to be lower in DCL compared to Mo-DC. In contrast to DCLs derived from WT hESCs, CP DCLs expressed lower levels of co-stimulatory molecules CD86, CD80, CD83, HLA Class II, CD40 and CCR7, which are known to activate T cells (Fig. 1b, 1c and S1c). Even after stimulation by a strong inflammatory cocktail containing LPS and TNF-α, DCLs derived from WT parental hESCs were activated and matured, but CP DCLs could not be activated with elevated expression levels of *CTLA4-Ig, PD-L1* and the immunosuppressive *HLA-G* molecule (Fig. 1b, S1d and S1e). These results indicate that the CP expression maintains the immune suppressive characteristics of DCLs even after robust inflammatory stimuli.

3.2. CP DCLs exhibit impaired capacity to activate naïve T cells and promote Treg cells

Based on the persistent tolerogenic phenotypes of CP DCLs, we hypothesized that CP DCLs could have immune suppressive effects on allogeneic T cells. To test this hypothesis, we examined the capacity of CP DCLs to activate naïve allogeneic $CD8^+$ and $CD4^+$ T cells. When compared to WT DCLs with or without prior TNF-α activation, CP DCLs showed reduced capacity to stimulate the proliferation of allogeneic $CD8^+$ and $CD4^+$T cells (Fig. 2a). As a control, we also performed the same experiments using Mo-DC (Fig.S2b). Following T cell activation, CD62L is shed from the cell membrane of $CD8^+$ T cells *[44]*. When compared to those of $CD8^+$ T cells co-cultured with WT DCLs, the CD62L levels on $CD8^+$ T cells co-cultured with CP DCLs were much higher and similar to those without co-culture with any DCLs (Fig. 2b). These findings indicate that, in contrast to WT DCLs, CP DCLs fail to activate allogeneic T cells.

To test the hypothesis that CP DCLs might induce immune tolerance by stimulating Treg cells, we examined the ability of CP DCLs to promote Treg cells in the co-culture of DCLs and allogeneic $CD4^+$ T cells. Our data demonstrate that CP DCLs can significantly increase the proportion of $CD25^{high}Foxp3^+CD4^+$ Treg cells and the expression levels of immune suppressive *CTLA4* and *LAG3* (Fig. 2c). These findings indicate that CP DCLs suppress the activation of $CD8^+$ T cell and promote the generation of Treg cells.

3.3. The adoptive transfer of CP DCLs protects parental hESC-derived allografts from immune rejection in vivo

Considering the immune suppressive characteristics of CP DCLs, we hypothesized that CP DCLs could induce immune tolerance of the parental hESC-derived allografts. To test this hypothesis, we used Hu-mice reconstituted with functional human immune system by the transplantation of human fetal thymic tissues under the kidney capsule and simultaneous intravenous injection of isogenic $CD34^+$ fetal liver cells into immunodeficient NSG ($NOD.Cg\text{-}Prkdc^{scid}Il2rg^{tm1Wjl}/SzJ$) mice, known also as BLT model *[43]*. These Hu-mice are well reconstituted with human T and B cells (Fig. S3), and are able to mount effective allogeneic immune rejection of hESC-derived cells *[22]*.

As hESCs can form teratomas that contain cells derived from all three germ layers, we tested whether CP DCLs could protect the parental hESC-derived teratomas from allogeneic immune rejection. While hESCs formed teratomas with similar kinetics in NSG and Hu-mice that received CP DCLs, teratomas formation was slower in Hu-mice that did not receive any CP DCLs, suggesting that the prior transplantation of CP DCLs can protect hESC-derived allografts from immune rejection (Fig. 3a). In support of this notion, the teratomas formed in Hu-mice that did not receive any CP DCLs were extensively infiltrated with T cells (Fig. 3b, 3c and S4a). In contrast, significantly fewer T cells were detected in teratomas formed in Hu-mice that received CP DCLs (Fig. 3b, 3c and S4a). In addition, when compared to that of teratomas formed in Hu-mice that did not receive any DCLs, the infiltration of other immune cells such as monocytes and B cells was also reduced in the teratomas formed in Hu-mice that received CP DCLs (Fig. 3d). The presence of NK cells couldn`t be detected in teratomas (Fig. S4b), suggesting that NK cells are unlikely involved directly in the immune rejection. Consistent with the findings of T cell infiltration, the expression of human *CD3* gene was lower in the teratomas of Hu-mice that received CP DCLs than those that didn`t receive any DCLs that (Fig. 3e). In addition, compared to those of Hu-mice that received no DCLs, the infiltrating T cells in the teratomas of Hu-mice that received CP DCLs expressed higher levels of *FOXP3* and immune suppressive cytokine such as *TGF-β* and *IL-10*, all markers of Treg cells (Fig. 3e and S4c). These results indicate that the prior transfusion of CP DCLs in Hu-mice can prevent the allogeneic immune rejection of the parental hESC-derived teratomas by inhibiting immune cell infiltration and promoting Treg cell dependent immune suppressive microenvironment.

3.4. CP DCLs protect parental hESC-derived cardiomyocytes from allogeneic immune rejection

To further confirm if CP DCLs can protect parental hESC-derived functional cells from allogeneic immune rejection, the parental hESCs were differentiated into cardiomyocytes and characterized (Fig. S5). Hu-mice with similar reconstitution levels of human immune system received intravenous injection of PBS control and DCLs derived from either WT or CP hESCs. At day 7 after DCL injection, cardiomyocytes differentiated from the parental hESCs were transplanted into the hindleg of the Hu-mice (Fig. 4a). As a control for graft survival, the same batch of cardiomyocytes was transplanted into the hindleg of the NSG mice. Grafts were collected 2 and 4 weeks after transplantation and analyzed for cardiomyocyte survival and T cell infiltration. Two weeks after transplantation, the survival rate of hESC-derived cardiomyocytes in Hu-mice with prior transplantation of CP DCLs was significantly higher than that in Hu-mice that received WT DCLs or did not receive any DCLs, and was comparable to that in NSG mice (Fig. 4b). Four weeks after transplantation, while Hu-mice that did not receive DCL injection completely rejected the grafted allogeneic cardiomyocytes, Hu-mice that received CP DCLs retained most of the grafted allogeneic cardiomyocytes (Fig. 4c and 4d). Hu-mice that

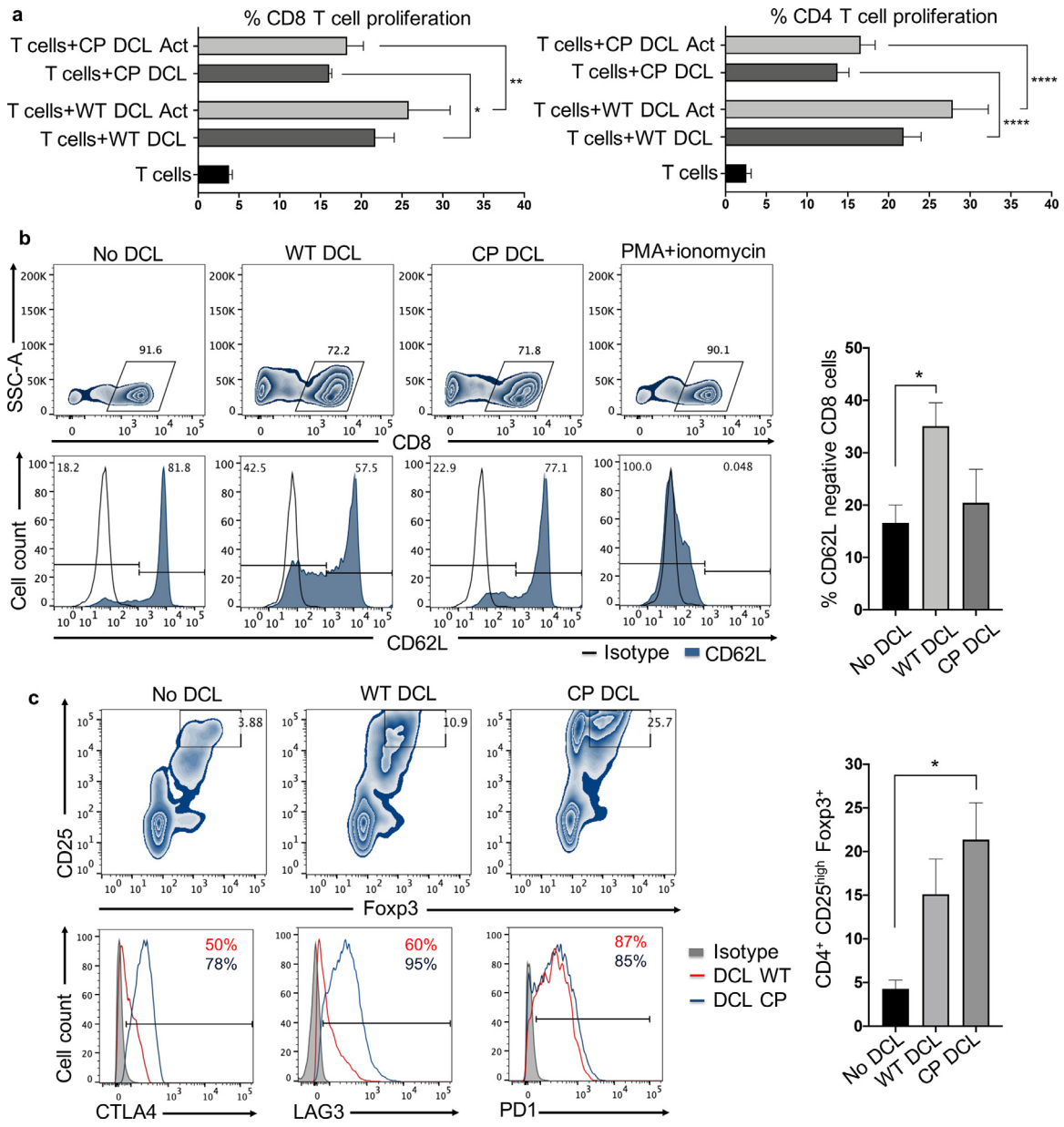

Fig. 2. CP DCL cells fail to activate T cells but promote Treg cells. (a) T cell proliferation was assessed in presence of immature or activated WT and CP DCL cells. $CD8^+$ and $CD4^+$ T cells were purified from spleens of Hu-mice and labeled with CFSE. 5×10^5 allogeneic $CD8^+$ or $CD4^+$ T cells were co-cultured with 1.25×10^5 hESC-derived DCL cells for 5 days. The percentage of $CD3^+CFSE^{low}$ T cells was quantified by flow cytometry and presented as mean values ± SEM ($n = 4$). Data from different groups were compared using one-way ANOVA test, *, ** and **** denote significant differences at $P<0.05$, $P<0.01$ and $P<0.0001$. (b) Allogeneic $CD8^+$ human T cells purified from spleens of Hu-mice were co-cultured with WT and CP DCL cells. The surface expression of CD62L by $CD8^+$ T cells was assessed by flow cytometry. The experiments were performed with 3 independent sets of DCL cells and $CD8^+$ T cells isolated from spleens of Hu-mice established with fetal tissues from 2 different donors. Data are presented as mean values ± SEM ($n = 3$). Data from different groups were compared using Kruskal-Wallis test with Dunn`s multiple comparison test, * $P<0.05$. (c) Allogeneic $CD4^+$ T cells purified from spleens of Hu-mice were co-cultured with WT and CP DCL cells for 7 days. The percentage of $CD25^{high}Foxp3^+$ $CD4^+$ T cells was assessed by flow cytometry and shown as mean values ± SEM ($n = 5$). Representative expression profile of CTLA4, LAG3 and PD1 by $CD25^{high}Foxp3^+$ $CD4^+$ T cells are shown. Data from different groups were compared using one-way ANOVA test, * $P<0.05$.

received WT DCLs retained approximately 20% of the cardiomyocyte allograft, which was not different from that in Hu-mice which did not receive any transfusion of DCLs (Fig. 4c and 4d).

Consistent with the survival data of cardiomyocyte allografts, T cell infiltration was significantly higher in the allografts of Hu-mice without DCL transfusion than in those of Hu-mice with CP DCL transfusion (Fig. 4b, 4c and 4d). T cell infiltration was slightly lower in the cardiomyocyte allografts of Hu-mice with prior WT DCL transfusion than in the cardiomyocyte allografts of Hu-mice without DCLs 2 weeks after cardiomyocyte transplantation (Fig.4b) but reached similar levels 4 weeks after transplantation (Fig.4c and 4d). By analyzing T cells infiltrating in the grafts for the presence of $FOXP3^+$ cells, we found significantly increased proportion of $FOXP3^+$ Treg cells in the grafts of Hu-mice that received CP DCLs than those without DCL transfusion (Fig. 4e). In contrast, the proportion of $CD25^{high}$-$FOXP3^+CD4^+$ T cells in the spleens of Hu-mice without prior DCL injection is similar to that in the spleens of the Hu-mice that received CP DCLs (Fig. 4f). These results indicate that CP DCLs can protect cardiomyocyte allografts from immune rejection by promoting the recruitment or expansion of Treg cells in the grafts.

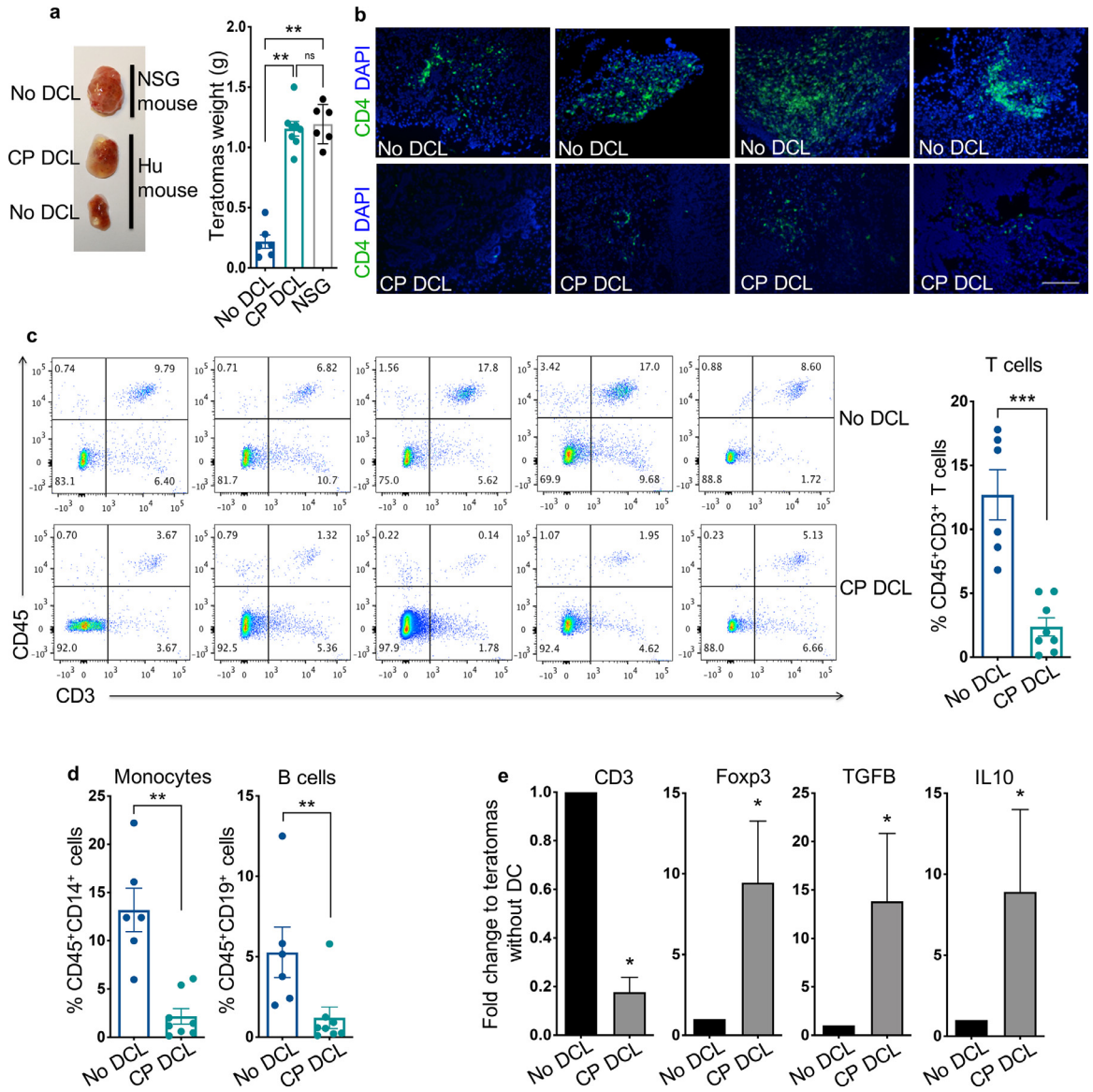

Fig. 3. CP DCL cells protect hESC-derived teratomas from allogeneic immune rejection. (a) Teratomas weight and representative image of teratomas formed by HUES3 hESCs in NSG mice, in Hu-mice injected with DCL cells differentiated from CP HUES3 ESCs (HUES3 CP DCL cells), and in Hu-mice that didn`t receive any DCL cells. The DCL cells were delivered via the tail vein 7 days prior to the subcutaneous transplantation of hESCs. Teratomas were collected 6 to 8 weeks after transplantation. No DCL group $n = 6$, CP DCL group $n = 8$, NSG group $n = 6$. Data are presented as mean values ± SEM. Data from different groups were compared using Kruskal-Wallis test with Dunn`s multiple comparison test, $^{**}p<0.01$. (b) Representative images of $CD4^+$ *T* cell infiltration into the HUES3 teratomas formed in Hu-mice with or without prior HUES3 CP DCL cell transplantation. The presence of $CD4^+$T cells was revealed by immunofluorescent staining. Scale bar 200 μm. (c) $CD3^+$ T cell infiltration into the HUES3 teratomas formed in Hu-mice with or without prior HUES3 CP DCL cell transplantation was evaluated by flow cytometry. The plots show representative data obtained from 5 different batches of Hu-mice (5 different donors of human fetal liver and thymus). No DCL group $n = 6$, CP DCL group $n = 8$. Data are presented as mean values ± SEM. The two groups were compared using non-parametric Mann-Whitney test. *** $p<0.001$. (d) The infiltration of human monocyte and B cells into the HUES3 teratomas formed in Hu-mice with or without prior HUES3 CP DCL cell transplantation. No DCL group $n = 6$, CP DCL group $n = 8$. Data are presented as mean values ± SEM. The two groups were compared using non-parametric Mann-Whitney test. ** $P<0.01$. (e) Relative expression of *CD3, FOXP3, TGFB and IL-10* genes in HUES3 teratomas formed in Hu-mice with or without prior HUES3 CP DCL cell transplantation. The levels of *CD3* mRNA were normalized with those of *GAPDH* mRNA, *FOXP3, TGFB* and *IL-10* mRNA levels were normalized with those of *CD3* mRNA. The fold change difference in gene expression was tested using Wilcoxon signed rank test, $n = 7$ for each group, * $P<0.05$.

3.5. CP DCLs protected the parental hESC-derived smooth muscle cells (SMCs) from allogeneic immune rejection but did not induce systemic immune suppression

To further confirm our conclusion, we tested the capability of CP DCLs to protect the parental hESC-derived SMCs (Fig. 5a) from allogeneic immune rejection. As described above, Hu-mice were intravenously injected with PBS or DCLs derived from either WT or CP hESCs. At day 7 after DCL transfusion, SMCs differentiated from the parental hESCs were transplanted into the hindleg muscle of the Hu-mice. The same batch of SMCs was transplanted into the hindlegs of NSG mice as a control for graft survival. The grafts were collected 2 weeks after transplantation and analyzed for graft survival and T cell infiltration. Consistent with the findings of hESC-derived cardiomyocytes, when compared to SMC allografts in Hu-mice with prior transfusion of WT DCLs or PBS, the prior transfusion of CP DCLs in Hu-mice significantly improved the survival of parental hESC-derived SMCs and reduced T cell infiltration into the allografts (Fig. 5b and 5c). In contrast to Hu-mice that received CP DCLs, robust T cell infiltration but few remaining SMCs were detected in Hu-mice that received WT DCLs or PBS (Fig. 5b and 5c). By analyzing T cells infiltrating in the grafts for the presence of $FOXP3^+$ cells, we found

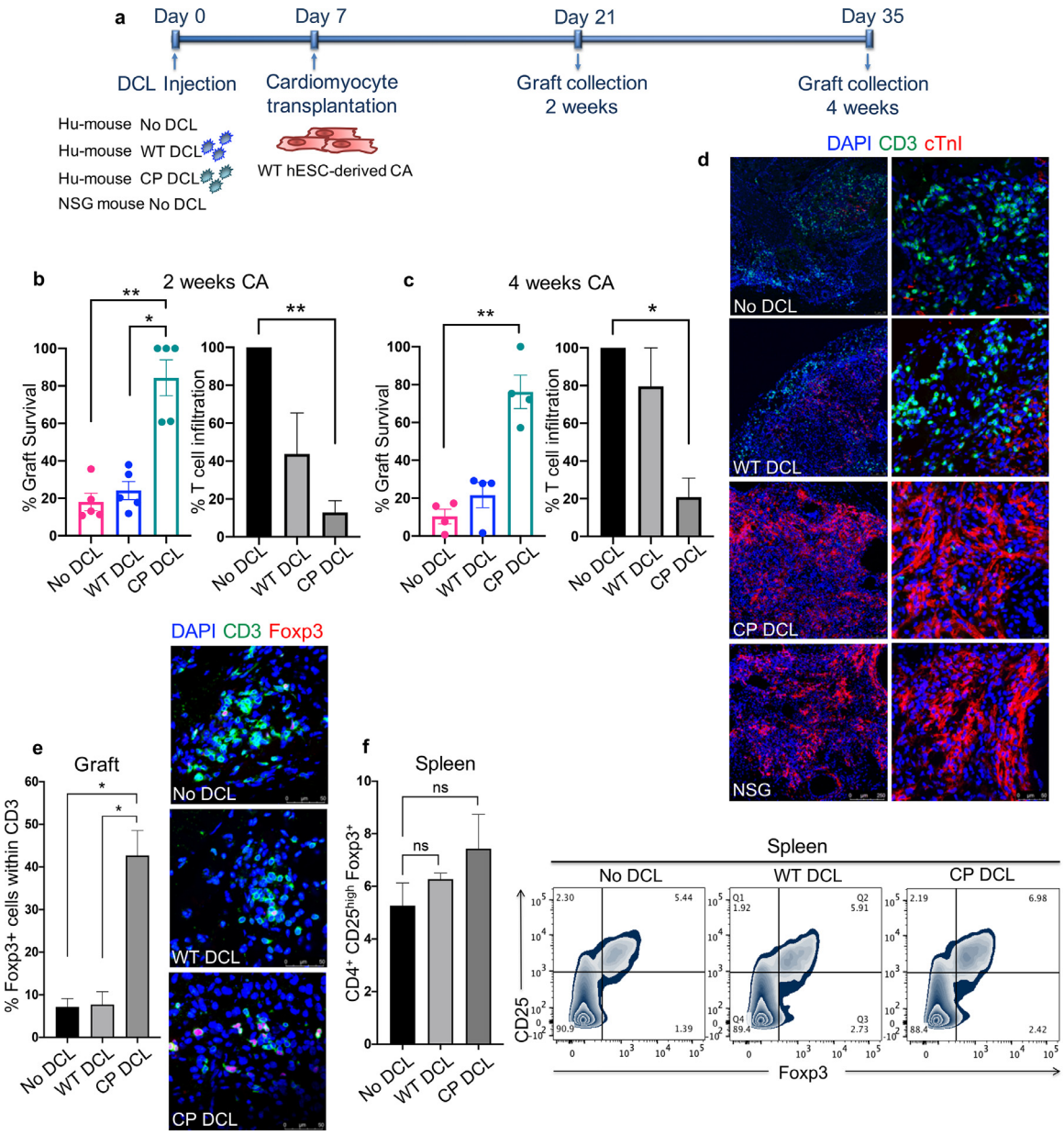

Fig. 4. CP DCL cells inhibit the allogeneic immune rejection of the same hESC line-derived cardiomyocytes in Hu-mice. (a) Schematic description of the experiments. DCL cells derived from WT and CP hESCs were delivered via the tail vein into Hu-mice. The experiments were performed using 2 different hESCs lines, H1 and HUES3. Seven days after intravenous injection of DCLs, the same hESC line-derived cardiomyocytes were transplanted into the skeletal muscle of Hu-mice and NSG control mice. (b) Cardiomyocyte survival and T cell infiltration into the cardiomyocyte graft 2 weeks after transplantation (n = 5, H1 n = 3, HUES3 n = 2). (c) Cardiomyocyte survival and T cell infiltration into the cardiomyocyte graft 4 weeks after transplantation (n = 4, H1 n = 2, HUES3 n = 2). Sections were stained with anti-CD3 (shown in green) and anti-CTnI (shown in red) antibodies. For each section, the numbers of $CD3^+$ T cells and CTnI cells were counted, 3 sections per graft were analyzed. The graft survival rate was calculated in comparison to the graft survival in NSG mice. The T cell infiltration rate was calculated in comparison to that of grafts in Hu-mice without any DCL cell injection. Data are presented as mean values ± SEM. Data from different groups were compared using one-way ANOVA test. *$P<0.05$, ** $P<0.01$. (d) Representative immunofluorescent images of cardiomyocyte grafts recovered 4 weeks after transplantation. Sections were stained with anti-CD3 (shown in green) and anti-CTnI (shown in red) antibodies. Scale bar 250 μm (left panel), scale bar 50 μm (right panel). (e) The presence of $CD3^+FOXP3^+$ T cells in the cardiomyocyte grafts 2 weeks after transplantation. Grafts were sectioned and stained with anti-CD3 (shown in green) and anti-FOXP3 (shown in red) antibodies. For each section, the numbers of $CD3^+$ T cells and $FOXP3^+$ cells were counted, 2 sections per graft were analyzed, scale bar 50 μm. No DCL n = 3, WT DCL n = 3, CP DCL n = 4. Data from different groups were compared using Kruskal-Wallis test with Dunn`s multiple comparison test, * $P<0.05$. (f) The presence of $CD4^+CD25^{high}Foxp3^+$ T cells in the spleens of the Hu-mice 2 weeks after transplantation were analyzed by flow cytometry (No DCL n = 4, WT DCL n = 3, CP DCL n = 5). Data are presented as mean values ± SEM. The groups were compared using non-parametric Mann-Whitney test. ns, non significant.

significantly increased proportion of $FOXP3^+$ Treg cells in the grafts of Hu-mice that received CP DCLs than those without DCL transfusion (Fig. 5d). Therefore, the prior transfusion of CP DCLs can efficiently protect the parental hESC-derived smooth muscle cell allografts from immune rejection.

To test the possibility that the protection of hESC-derived allografts by CP DCLs is due to the induction of systemic immune suppression, CP DCLs derived from HUES3 CP hESCs, denoted HUES3 CP DCLs, were intravenously transfused into Hu-mice. At day 7 after injection, HUES3 hESCs were transplanted subcutaneously into the left flank and H9 hESCs into the right flank of the same Hu-mice. The same batch of hESCs was transplanted into left and right flanks of the same NSG mice as the control for their capability to form teratoma. While HUES3 hESCs formed teratomas with similar kinetics and sizes

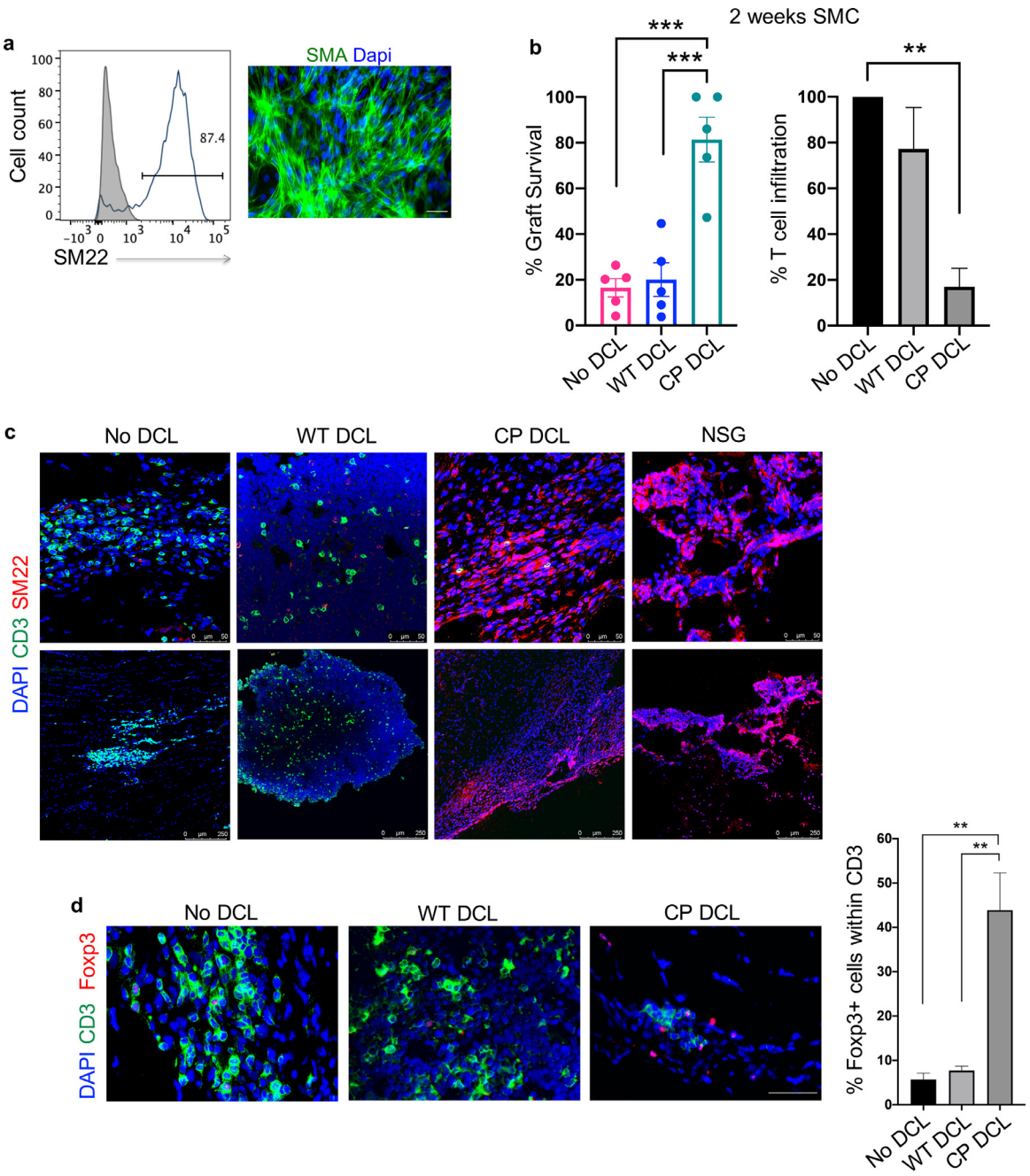

Fig. 5. CP DCL cells inhibit the allogeneic immune rejection of the same hESC line-derived smooth muscle cells in Hu-mice. (a) Characterization of hESC-derived smooth muscle cells (SMCs). The expression of SM22 was analyzed by Flow cytometry and immunofluorescence microscopy, scale bar 50 μm. (b) SMC survival and T cell infiltration in the grafts 2 weeks after transplantation. Seven days after intravenous injection of DCLs, the same hESC line-derived SMCs were transplanted into the skeletal muscle of Hu-mice and NSG control mice (n = 5). Data are presented as mean values ± SEM. Data from different groups were compared using one-way ANOVA test. $^{**}p<0.01$, $^{***}p<0.001$. (c) Representative immunofluorescent staining of SMC grafts 2 weeks after transplantation. Sections were stained with anti-CD3 (shown in green) and anti-SM22 (shown in red) antibodies. Scale bar 50 μm (upper panel), scale bar 250 μm (lower panel).(d) The presence of $CD3^+FOXP3^+$ T cells in the smooth muscle cell grafts 2 weeks after transplantation. Grafts were sectioned and stained with anti-CD3 (shown in green) and anti-FOXP3 (shown in red) antibodies. For each section, the numbers of $CD3^+$ T cells and $FOXP3^+$ cells were counted, 2 sections per graft were analyzed, scale bar 50 μm. No DCL n = 4, WT DCL n = 4, CP DCL n = 3. Data from different groups were compared using one-way ANOVA test, $^{**}p<0.01$.

in Hu-mice and NSG mice, the teratomas formed by H9 WT hESCs in Hu-mice were much smaller than those formed in NSG mice and exhibited extensive necrosis and T cell infiltration (Fig. S6a-d), indicating that the prior transfusion of CP DCLs can selectively protect HUES3 hESC-derived allografts but not H9 hESC-derived allografts from allogeneic immune rejection. In further support of this conclusion, prior transfusion of CP DCLs into Hu-mice selectively protected the parental hESC-derived SMCs but not non-parental hESC-derived SMCs from allogeneic immune rejection (Fig. S7 a, b and c). Therefore, the prior transfusion of CP DCLs does not cause systemic immune suppression but induce immune tolerance specifically to the parental hESC-derived allografts. In this context, only T cells specific for the DCL-expressing HLAs are immune tolerated, while other T cells would remain able to mount immune responses to antigens produced during infection or cellular transformation, improving the safety of the immune tolerance strategy.

3.6. DCLs have short survival in Hu-mice

To distinguish the possibilities that CP DCLs induce immune protection or immune tolerance of parental hESC-derived allografts, we examined the survival of DCLs in Hu-mice after intravenous injection into Hu-mice. WT and CP DCLs were labeled using Vybrant CFDA SE cell tracer kit and injected into the tail vein of Hu-mice. At different time points after transfusion, the blood, spleen and thymus were collected and analyzed by flow cytometry for the presence of CFDA-labeled DCLs (Fig. 6a). Day 2 after injection, both WT and CP DCLs were detected in the spleen of Hu-mice (Fig. 6b and 6c). Day 7 after injection, DCLs were still detected in the spleen, but not in the thymus or the blood of Hu-mice (Fig. 6b-d). Although both injected DCLs were detected at very low levels in the spleens of Hu-mice, the percentage of CP DCLs was significantly higher than that of WT DCLs. Day 10 after injection, very few DCLs could be detected in the spleens of Hu-mice (Fig. 6b). Therefore, CP DCLs can only stay for a short period of time in Hu-mice, but can induce long-term immune tolerance of parental hESC-derived allografts.

4. Discussion

Despite significant progress in developing hESC-based therapies to treat major human diseases, one of the key challenges remains the allogeneic immune rejection of hESC-derived allografts [45]. While the typical immune suppressants can effectively prevent allogeneic immune rejection, they pose serious infection and cancer risks for hESC-based therapy of chronic diseases such as macular degeneration and type 1 diabetes. This increases the risk versus benefit ratio of hESC-based cell therapy and thus reduces the feasibility of its clinical

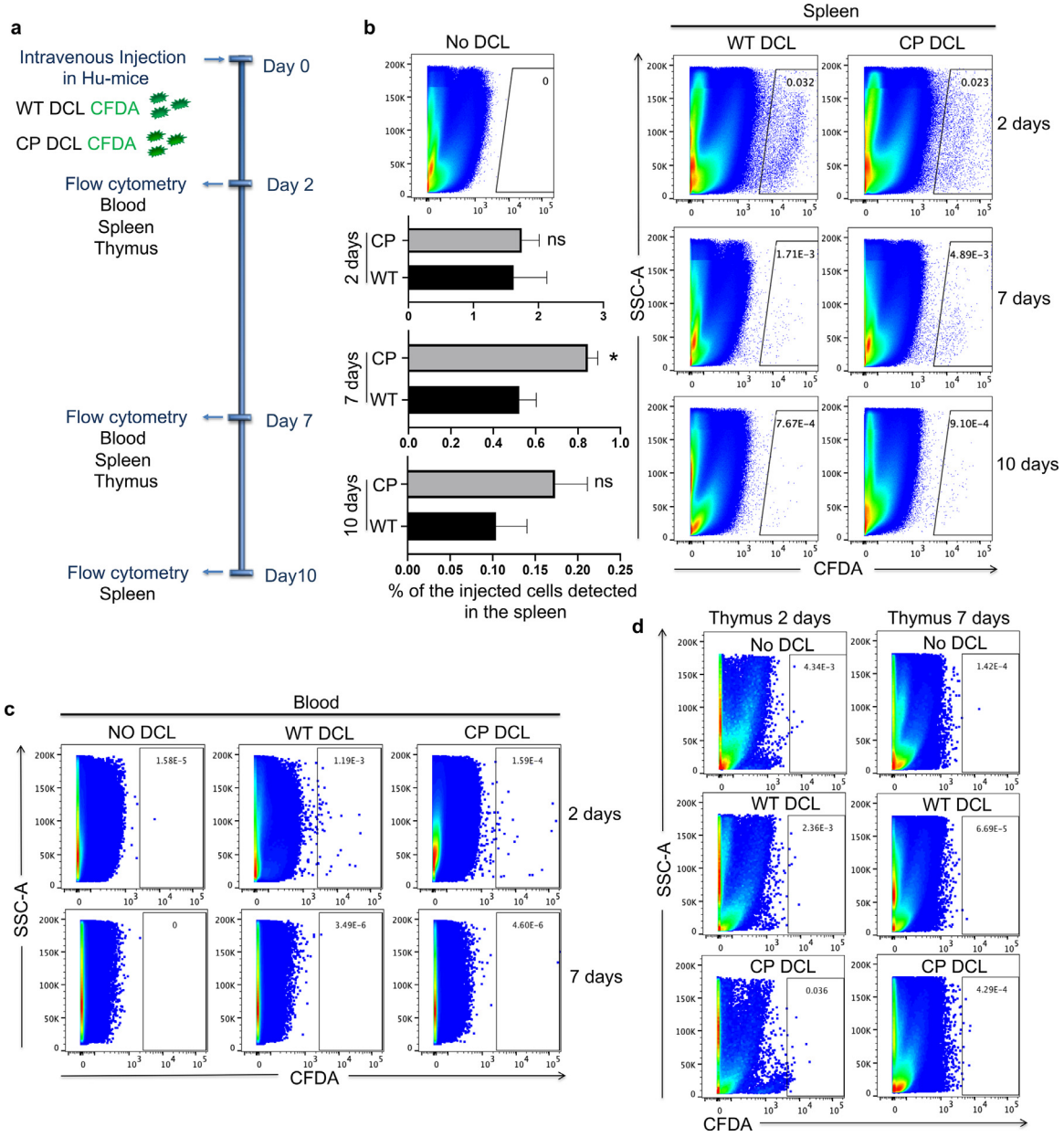

Fig. 6. The survival of hESC-derived DCL cells in Hu-mice. (a) Schematic description of the *in vivo* tracking of DCL cells. WT and CP DCL cells were labeled with CFDA and injected into the tail vein of Hu-mice. Two days, seven days and ten days after injection, the blood, spleen and thymus were collected and analyzed by flow cytometry for the presence of DCL cells. Hu-mice that didn`t receive any DCL cells were ered as controls. (b) The detection of WT and CP DCL cells in the spleen by flow cytometry. The data from the two groups were compared using the non-parametric Mann-Whitney test, * $P<0.05$. (c, d) The detection of WT and CP DCL cells in the blood (c) and (d) thymus by flow cytometry.

application. Various approaches have been published to prevent allogeneic immune rejection of hESC-derived allografts. For example, previous studies have shown that using CTLA4-Ig and anti-CD40 Ligand antibody could protect hESC-derived xenografts from mouse immune system [18]. While this approach remains to be validated in a model with functional human immune system, it will cause systemic immune suppression similarly to the standard immune suppressants. Secondly, the overexpression of CTLA4-Ig and PD-L1 in hESC-derived allografts can protect them from allogeneic immune rejection [22], but renders the hESC-derived allografts immune evasive and susceptible to infection and cancer. In addition, the expression of CTLA4-Ig and PD-L1 could affect the differentiation and function of hESC-derived cells. Thirdly, the knockout of HLA class I and II in hESCs using CRISPR/CAS9 technology could protect their derivatives from allogeneic T cells *in vitro* and in mouse models with human T cells [19–21]. One potential risk of this approach is that the CRISPR/CAS9 technology can induce genetic instability in the cells by disrupting the non-homologous end joining pathway [46]. In addition, the HLAI/II knockout cells are prone to infection and caner.

To develop a safe and effective approach to induce immune tolerance of hESC-derived allografts without the safety risk associated with previous approaches, we took advantage of the well-known capability of immature DCs to induce immune tolerance of antigen-specific T cells [29,47]. We demonstrate that CTLA4-Ig/PD-L1 expressing DCLs derived from hESCs can induce persistent immune tolerance of the parental hESC-derived allografts. There are many unique properties of CP DCLs that improve their capability to induce long-term immune tolerance. First, in contrast to normal immature DCs, the expression of CP ensures that CP DCLs remain immature and with tolerogenic properties even after strong inflammatory stimuli. Second, CP DCLs derived from hESCs enable the immune tolerance of T cells reactive to the alloantigens expressed by the cells derived from the same strain of hESCs. Thirdly, while CP DCLs survive briefly *in vivo*, they can induce long-term immune tolerance of parental hESC-derived allografts. This reduces the cancer risk of the genetically modified CP DCLs as well as parental hESC-derived allografts that remain under immune surveillance.

When compared to the published immune protection approaches that can either lead to systemic immune suppression or the establishment of immune evasive grafts, our approach will not lead to systemic immune suppression nor immune evasive allografts, and thus mitigate the cancer and infection risk associated with existing approaches. In this context, only T cells specific for the DCL-expressing alloantigens are immune tolerated, while other T cells remain able to mount immune responses to antigens produced during infection or cellular transformation. Based on the findings that CP DCLs can induce immune tolerance of various functional cell types derived from the same strain of hESCs, our approach should improve the feasibility for clinical development of hESC-based therapy. In this context, for each clinically approved hESC cell line, the development of CP hESC-derived DCLs can be universally applied to induce immune tolerance of various hESC-derived functional cells to treat various human diseases.

4.1. Caveats and limitations

Although these results are promising, our study has some important limitations. We show that CP DCLs can promote Treg cell *in vitro* and protect the allografts from immune rejection by promoting the recruitment or expansion of Treg cells in the grafts. However further in-depth study is warranted to better understand the mechanism by which CP DCLs induce immune tolerance. We conducted graft survival surveillance for up to 4 weeks but the question whether CP DCLs can protect the hESC-derived allografts for longer period of time needs to be addressed. As the immune microenvironment of the transplantation site plays an important role in shaping the immune response towards the graft [48], further studies are necessary to evaluate the efficiency of CP DCLs to promote tolerance towards hESCs-derived cells transplanted in different anatomical sites. In addition, although the DCLs generated in this study displays many of the characteristics of bona fide DCs, the improvement of the differentiation protocols to achieve clinical grade DCs is of critical importance to enable their clinical application. Our choice of differentiation protocol was based on previous published protocols for the differentiation of DCs from hPSCs [5,41] and previous studies that were able to successfully produce DCs with tolerogenic properties using GM-CSF and Il-4 [35,40,49]. However, it would be necessary to test if using other factors, such as Flt-3-ligand, would generate DCLs with better tolerogenic properties.

5. Data sharing

The related data and materials are available for sharing upon written request to the corresponding authors with signed material transfer agreement.

6. Contributors

Conceptualization, D.T., X.F., and Y.X.; Methodology, D.T., X.F., and Y.X.; Formal Analysis, D.T., X.F., and Y.X.; Investigation, D.T., Y.Z., Q.C., J.L., J.H.; Resources, F.X. and Y.X.; Writing – Original Draft, D.T., X.F., and Y.X.; Writing – Review & Editing, all authors; Supervision, X.F. and Y.X.; Project Administration, X.F. and Y.X.; Funding Acquisition X. F. and Y.X. All authors read and approved the final version of the manuscript.

Declaration of Competing Interest

The authors declare no competing interests.

Acknowledgments

This work was supported by the National Natural Science Foundation of China (No. 91959204, 81930084, 815300045, 81871197, U1601222), the leading talents of Guangdong Province Program (No. 00201516), the Key Research and Development Program of Guangdong Province (2019B020235003), Science and Technology Innovation Committee of Shenzhen Municipality (JCYJ20180504170301309), Shenzhen "Sanming" Project of Medicine (SZSM201602102), the National High-tech R&D Program (863 Program No. 2015AA020310), Development and Reform Commission of Shenzhen Municipality (S2016004730009), and a grant from CIRM (DISC2–10559).

Supplementary materials

Supplementary material associated with this article can be found, in the online version, at doi:10.1016/j.ebiom.2020.103120.

References

[1] Lian X, Hsiao C, Wilson G, Zhu K, Hazeltine LB, Azarin SM, et al. Robust cardiomyocyte differentiation from human pluripotent stem cells via temporal modulation of canonical Wnt signaling. Proc Natl Acad Sci U S A 2012;109:E1848–57. doi: 10.1073/pnas.1200250109.

[2] Nair GG, Liu JS, Russ HA, Tran S, Saxton MS, Chen R, et al. Recapitulating endocrine cell clustering in culture promotes maturation of human stem-cell-derived β cells. Nat Cell Biol 2019;21:263–74. doi: 10.1038/s41556-018-0271-4.

[3] Pagliuca FW, Millman JR, Gürtler M, Segel M, Van Dervort A, Ryu JH, et al. Generation of functional human pancreatic β cells in vitro. Cell 2014;159:428–39. doi: 10.1016/j.cell.2014.09.040.

[4] Patsch C, Challet-Meylan L, Thoma EC, Urich E, Heckel T, O'Sullivan JF, et al. Generation of vascular endothelial and smooth muscle cells from human pluripotent stem cells. Nat Cell Biol 2015;17:994–1003. doi: 10.1038/ncb3205.

[5] Senju S, Haruta M, Matsumura K, Matsunaga Y, Fukushima S, Ikeda T, et al. Generation of dendritic cells and macrophages from human induced pluripotent stem cells aiming at cell therapy. Gene Ther 2011;18:874–83. doi: 10.1038/gt.2011.22.

[6] Stacpoole SRL, Bilican B, Webber DJ, Luzhynskaya A, He XL, Compston A, et al. Efficient derivation of NPCs, spinal motor neurons and midbrain dopaminergic neurons from hESCs at 3% oxygen. Nat Protoc 2011;6:1229–40. doi: 10.1038/nprot.2011.380.

[7] Menasché P, Vanneaux V, Hagège A, Bel A, Cholley B, Parouchev A, et al. Transplantation of human embryonic stem cell-derived cardiovascular progenitors for severe ischemic left ventricular dysfunction. J Am Coll Cardiol 2018;71:429–38. doi: 10.1016/j.jacc.2017.11.047.

[8] Schwartz SD, Regillo CD, Lam BL, Eliott D, Rosenfeld PJ, Gregori NZ, et al. Human embryonic stem cell-derived retinal pigment epithelium in patients with age-related macular degeneration and Stargardt's macular dystrophy: follow-up of two open-label phase 1/2 studies. Lancet Lond Engl 2015;385:509–16. doi: 10.1016/S0140-6736(14)61376-3.

[9] Wirth III E, Lebkowski JS, Lebacqz K. Response to frederic Bretzner et al. "Target populations for first-in-human embryonic stem cell research in spinal cord injury. Cell Stem Cell 2011;8:476–8. doi: 10.1016/j.stem.2011.04.008.

[10] Blair NF, Barker RA. Making it personal: the prospects for autologous pluripotent stem cell-derived therapies. Regen Med 2016;11:423–5. doi: 10.2217/rme-2016-0057.

[11] Chakradhar S. An eye to the future: researchers debate best path for stem cell-derived therapies. Nat Med 2016;22:116–9. doi: 10.1038/nm0216-116.

[12] Deuse T, Hu X, Agbor-Enoh S, Koch M, Spitzer MH, Gravina A, et al. De novo mutations in mitochondrial DNA of iPSCs produce immunogenic neoepitopes in mice and humans. Nat Biotechnol 2019;37:1137–44. doi: 10.1038/s41587-019-0227-7.

[13] Zhao T, Zhang Z-N, Rong Z, Xu Y. Immunogenicity of induced pluripotent stem cells. Nature 2011;474:212–5. doi: 10.1038/nature10135.

[14] Zhao T, Zhang Z, Westenskow PD, Todorova D, Hu Z, Lin T, et al. Humanized mice reveal differential immunogenicity of cells derived from autologous induced pluripotent stem cells. Cell Stem Cell 2015;17:353–9. doi: 10.1016/j.stem.2015.07.021.

[15] Boyd AS, Rodrigues NP, Lui KO, Fu X, Xu Y. Concise review: Immune recognition of induced pluripotent stem cells. Stem Cells Dayt Ohio 2012;30:797–803. doi: 10.1002/stem.1066.

[16] Lindenfeld J, Miller GG, Shakar SF, Zolty R, Lowes BD, Wolfel EE, et al. Drug therapy in the heart transplant recipient part II: immunosuppressive drugs. Circulation 2004;110:3858–65. doi: 10.1161/01.CIR.0000150332.42276.69.

[17] Lui KO, Howie D, Ng SW, Liu S, Chien KR, Waldmann H. Tolerance induction to human stem cell transplants with extension to their differentiated progeny. Nat Commun 2014;5:5629. doi: 10.1038/ncomms6629.

[18] Szot GL, Yadav M, Lang J, Kroon E, Kerr J, Kadoya K, et al. Tolerance induction and reversal of diabetes in mice transplanted with human embryonic stem cell-derived pancreatic endoderm. Cell Stem Cell 2015;16:148–57. doi: 10.1016/j.stem.2014.12.001.

[19] Deuse T, Hu X, Gravina A, Wang D, Tediashvili G, De C, et al. Hypoimmunogenic derivatives of induced pluripotent stem cells evade immune rejection in fully immunocompetent allogeneic recipients. Nat Biotechnol 2019;37:252–8. doi: 10.1038/s41587-019-0016-3.

[20] Gornalusse GG, Hirata RK, Funk SE, Riolobos L, Lopes VS, Manske G, et al. HLA-E-expressing pluripotent stem cells escape allogeneic responses and lysis by NK cells. Nat Biotechnol 2017;35:765–72. doi: 10.1038/nbt.3860.

[21] Xu H, Wang B, Ono M, Kagita A, Fujii K, Sasakawa N, et al. Targeted disruption of HLA genes via CRISPR-Cas9 generates iPSCs with enhanced immune compatibility. Cell Stem Cell 2019;24:566–78 e7. doi: 10.1016/j.stem.2019.02.005.

[22] Rong Z, Wang M, Hu Z, Stradner M, Zhu S, Kong H, et al. An effective approach to prevent immune rejection of human ESC-derived allografts. Cell Stem Cell 2014;14:121–30. doi: 10.1016/j.stem.2013.11.014.

[23] Okazaki T, Honjo T. The PD-1-PD-L pathway in immunological tolerance. Trends Immunol 2006;27:195–201. doi: 10.1016/j.it.2006.02.001.

[24] Walker LSK, Sansom DM. The emerging role of CTLA4 as a cell-extrinsic regulator of T cell responses. Nat Rev Immunol 2011;11:852–63. doi: 10.1038/nri3108.

[25] Bluestone JA, St. Clair EW, Turka LA. CTLA4Ig: bridging the basic immunology with clinical application. Immunity 2006;24:233–8. doi: 10.1016/j.immuni.2006.03.001.

[26] Morelli AE, Thomson AW. Tolerogenic dendritic cells and the quest for transplant tolerance. Nat Rev Immunol 2007;7:610–21. doi: 10.1038/nri2132.

[27] Gotsman I, Sharpe AH, Lichtman AH. T cell costimulation and coinhibition in atherosclerosis. Circ Res 2008;103:1220–31. doi: 10.1161/CIRCRESAHA.108.182428.

[28] Jonuleit H, Schmitt E, Steinbrink K, Enk AH. Dendritic cells as a tool to induce anergic and regulatory T cells. Trends Immunol 2001;22:394–400.

[29] Ezzelarab M, Thomson AW. Tolerogenic dendritic cells and their role in transplantation. Semin Immunol 2011;23:252–63. doi: 10.1016/j.smim.2011.06.007.

[30] Hackstein H, Thomson AW. Dendritic cells: emerging pharmacological targets of immunosuppressive drugs. Nat Rev Immunol 2004;4:24–34. doi: 10.1038/nri1256.

[31] Kitajima T, Ariizumi K, Bergstresser PR, Takashima A. A novel mechanism of glucocorticoid-induced immune suppression: the inhibiton of T cell-mediated terminal maturation of a murine dendritic cell line. J Clin Invest 1996;98:142–7. doi: 10.1172/JCI118759.

[32] Li M, Zhang X, Zheng X, Lian D, Zhang Z-X, Ge W, et al. Immune modulation and tolerance induction by RelB-silenced dendritic cells through RNA interference. J Immunol Baltim Md 1950 2007;178:5480–7. doi: 10.4049/jimmunol.178.9.5480.

[33] Rutella S, Danese S, Leone G. Tolerogenic dendritic cells: cytokine modulation comes of age. Blood 2006;108:1435–40. doi: 10.1182/blood-2006-03-006403.

[34] Tan PH, Sagoo P, Chan C, Yates JB, Campbell J, Beutelspacher SC, et al. Inhibition of NF-kappa B and oxidative pathways in human dendritic cells by antioxidative vitamins generates regulatory T cells. J Immunol Baltim Md 1950 2005;174:7633–44.

[35] Bonham CA, Peng L, Liang X, Chen Z, Wang L, Ma L, et al. Marked prolongation of cardiac allograft survival by dendritic cells genetically engineered with NF-kappa B oligodeoxyribonucleotide decoys and adenoviral vectors encoding CTLA4-Ig. J Immunol Baltim Md 1950 2002;169:3382–91. doi: 10.4049/jimmunol.169.6.3382.

[36] Min WP, Gorczynski R, Huang XY, Kushida M, Kim P, Obataki M, et al. Dendritic cells genetically engineered to express Fas ligand induce donor-specific hyporesponsiveness and prolong allograft survival. J Immunol Baltim Md 1950 2000;164:161–7. doi: 10.4049/jimmunol.164.1.161.

[37] Ezzelarab MB, Zahorchak AF, Lu L, Morelli AE, Chalasani G, Demetris AJ, et al. Regulatory dendritic cell infusion prolongs kidney allograft survival in nonhuman primates. Am J Transplant Off J Am Soc Transplant Am Soc Transpl Surg 2013;13:1989–2005. doi: 10.1111/ajt.12310.

[38] Thomson AW, Humar A, Lakkis FG, Metes DM. Regulatory dendritic cells for promotion of liver transplant operational tolerance: Rationale for a clinical trial and accompanying mechanistic studies. Hum Immunol 2018;79:314–21. doi: 10.1016/j.humimm.2017.10.017.

[39] Cai S, Hou J, Fujino M, Zhang Q, Ichimaru N, Takahara S, et al. iPSC-derived regulatory dendritic cells inhibit allograft rejection by generating alloantigen-specific regulatory T cells. Stem Cell Rep 2017;8:1174–89. doi: 10.1016/j.stemcr.2017.03.020.

[40] Sachamitr P, Leishman AJ, Davies TJ, Fairchild PJ. Directed differentiation of human induced pluripotent stem cells into dendritic cells displaying tolerogenic properties and resembling the CD141+ subset. Front Immunol 2017;8:1935. doi: 10.3389/fimmu.2017.01935.

[41] Choi K-D, Vodyanik M, Slukvin II. Hematopoietic differentiation and production of mature myeloid cells from human pluripotent stem cells. Nat Protoc 2011;6:296–313. doi: 10.1038/nprot.2010.184.

[42] Huang H, Zhao X, Chen L, Xu C, Yao X, Lu Y, et al. Differentiation of human embryonic stem cells into smooth muscle cells in adherent monolayer culture. Biochem Biophys Res Commun 2006;351:321–7. doi: 10.1016/j.bbrc.2006.09.171.

[43] Lan P, Tonomura N, Shimizu A, Wang S, Yang Y-G. Reconstitution of a functional human immune system in immunodeficient mice through combined human fetal thymus/liver and CD34+ cell transplantation. Blood 2006;108:487–92. doi: 10.1182/blood-2005-11-4388.

[44] Yang S, Liu F, Wang QJ, Rosenberg SA, Morgan RA. The shedding of CD62L (L-selectin) regulates the acquisition of lytic activity in human tumor reactive T lymphocytes. PloS One 2011;6:e22560. doi: 10.1371/journal.pone.0022560.

[45] Fu X, Xu Y. Challenges to the clinical application of pluripotent stem cells: towards genomic and functional stability. Genome Med 2012;4:55. doi: 10.1186/gm354.

[46] Xu S, Kim J, Tang Q, Chen Q, Liu J, Xu Y, et al. CAS9 is a genome mutator by directly disrupting DNA-PK dependent DNA repair pathway. Protein Cell 2020. doi: 10.1007/s13238-020-00699-6.

[47] Thomson AW, Ezzelarab MB. Regulatory dendritic cells: profiling, targeting, and therapeutic application. Curr Opin Organ Transplant 2018;23:538–45. doi: 10.1097/MOT.0000000000000565.

[48] Todorova D, Kim J, Hamzeinejad S, He J, Xu Y. Brief report: immune microenvironment determines the immunogenicity of induced pluripotent stem cell derivatives. Stem Cells Dayt Ohio 2016;34:510–5. doi: 10.1002/stem.2227.

[49] Dhodapkar MV, Steinman RM. Antigen-bearing immature dendritic cells induce peptide-specific CD8(+) regulatory T cells in vivo in humans. Blood 2002;100:174–7. doi: 10.1182/blood.v100.1.174.